PERGAMON

International Journal of Solids and Structures 38 (2001) 7627–7641

INTERNATIONAL JOURNAL OF SOLIDS and STRUCTURES

www.elsevier.com/locate/ijsolstr

Modeling of moisture diffusion in the presence of bi-axial damage in polymer matrix composite laminates

Samit Roy [a,*], Weiqun Xu [a], Sneha Patel [b], Scott Case [b]

[a] Department of Mechanical Engineering, University of Missouri-Rolla, 1870 Miner Circle, Rolla, MO 65409-0050, USA
[b] Department of Engineering Science and Mechanics, Virginia Polytechnic Institute and State University, Blacksburg, VA 24061-0219, USA

Received 12 January 2000

Abstract

It is now well known that Fick's Law is frequently inadequate for describing moisture diffusion in polymers and polymer composites. Non-Fickian or anomalous diffusion is likely to occur when a polymer composite laminate is subjected to external stresses that could give rise to internal damage in the form of matrix cracks. As a result, it is necessary to take into account the combined effects of temperature, stress (or strain), and damage in the construction of such a model. In this paper, a modeling methodology based on irreversible thermodynamics applied within the framework of composite macro-mechanics is extended to the case of a bi-axially damaged laminate. The model allows characterization of non-Fickian diffusion coefficients as well as moisture saturation level from moisture weight gain data for laminates with pre-existing and non-evolving damage. A symmetric damage tensor based on continuum damage mechanics is incorporated in this model by invoking the principle of invariance with respect to coordinate transformations. For tractability, the diffusion governing equations are simplified for the special case of a laminate with bi-axially oriented matrix cracks that is subjected to a uniaxial tensile stress. The final equations obtained from this derivation indicate that both effective diffusivity and maximum saturation level for this particular case can be expressed as quadratic functions of crack density. Comparisons with test data for a bi-axially damaged AS4/PR500 graphite/epoxy woven composite are provided for model verifications. © 2001 Elsevier Science Ltd. All rights reserved.

Keywords: Bi-axial damage; Diffusion; Diffusivity; Maximum saturation level; Woven fabric composite laminate; Modeling; Characterization

---

1. Introduction

Although thousands of polymer matrix composite (PMC) components are currently in service in the aerospace industry as well as in civil infrastructure repair and rehabilitation, barriers still exist to further implementation in more structurally critical and extreme temperature applications. Most of these barriers

---

[*] Corresponding author. Tel.: +1-573-341-4313; fax: +1-573-341-4607.
E-mail address: sroy@umr.edu (S. Roy).

PII: S0020-7683(01)00021-X

are associated with the inability to accurately predict component lives, and therefore, component life cycle costs. A fiber reinforced composite material with a polymer matrix will typically absorb moisture in a humid environment and at elevated temperatures. Combined exposure to heat and moisture affects a PMC in a variety of ways. First, the hygrothermal swelling causes a change in the residual stresses within the composite that could lead to micro-crack formation. These micro-cracks in turn provide fast diffusion paths and thus alter the moisture absorption characteristics of the laminate. Secondly, heat and humidity may cause the matrix to become plasticized thus causing an increase in the strain to failure of the matrix. Thirdly, the chemical bond at the interface between fiber and matrix may be affected which in turn would influence strength and toughness. Finally, in the event of cyclic heating and cooling with a sustained use-temperature above the boiling point of water, vaporization and out-gassing of absorbed moisture may take place leading to physical damage and chemical changes within the PMC, especially at temperatures greater than the glass transition temperature (T_g) of the matrix. Continuous exposure to high moisture concentrations at the exposed surfaces of a PMC component could also lead to damage in the form of matrix cracking, dissolution, and peeling.

It is now widely recognized that cyclic moisture absorption and desorption plays a significant role in influencing the mechanical behavior, and therefore, long-term durability of polymers and PMC. Numerous diffusion models have been proposed over the years for modeling hygrothermal effects in PMC. The one most frequently used by researchers is the one-dimensional Fickian model. Unfortunately, this model tends to overestimate the moisture absorption in panels for short diffusion time (Shen and Springer, 1981). Some researchers have suggested that the deviation can be explained by a two-stage Fickian process (Gurtin and Yatomi, 1979; Carter and Kibler, 1978). Others claim that the diffusion process in a PMC is non-Fickian (Shirrell et al., 1979; Weitsman, 1991). In reality, the nature of the diffusion process depends on the material and on the environmental conditions that the material is exposed to. For example, if the rate of viscoelastic relaxation in a polymer is comparable to the rate of moisture diffusion, then the diffusion is likely to be non-Fickian. In addition, the presence of strong temperature and stress gradients has been known to engender non-Fickian driving forces. The presence of damage in the form of matrix cracks is very likely to result in anomalous diffusion. Employing a rigorous thermodynamic approach, Weitsman (1987) developed a model for coupled damage and moisture transport in a transversely isotropic, fiber reinforced polymer composite. The damage entity was represented as a skew-symmetric tensor and was included in the model as an internal state variable. However, the model was mathematically complex and was not amenable to a simple closed-form solution. Recently, Roy and Xu (2001) developed a similar model employing theory of irreversible thermodynamics within the framework of macro (continuum) mechanics to derive governing equations for diffusion in a PMC from first principles. A special form for Gibbs potential was formulated for an orthotropic material using stress, temperature, damage, and moisture concentration as independent state variables. A symmetric damage tensor originally proposed by Talreja (1994) was used for this purpose. The resulting governing equations incorporated coupled interactions between stress, temperature, damage, and moisture concentration on the diffusion process within an orthotropic material. For model validation, the model predictions were compared with experimental data for the special case of isothermal diffusion in an unstressed graphite/epoxy 5-harness satin woven laminate with pre-existing uniaxial damage.

The primary focus of this paper is to extend the uniaxial model previously presented (Roy and Xu, 2001) to include pre-existing bi-axial states of damage. In addition to predicting changes in laminate diffusion coefficient with the degree of damage, the proposed model also allows characterization and prediction of moisture saturation levels from moisture weight gain data for laminates with pre-existing damage. Damage evolution is not included in the present analysis in the interest of tractability. This approach provides a significant improvement over methods reported in the literature for problems of this nature. For model validation, the model predictions are compared with experimental data for the special case of isothermal diffusion in an unstressed 5-harness satin woven laminate with pre-existing bi-axial damage states.

2. Model development

The Gibbs potential for an orthotropic material subjected to applied stress and internal damage must be expressed in a polynomial form that remains invariant to coordinate transformations. Such a polynomial can be mathematically expressed as a combination of invariant terms obtained from the so-called irreducible integrity bases (Talreja, 1994; Adkins, 1959). The irreducible integrity bases for orthotropic materials are,

$$\begin{gathered}\bar{\sigma}_{11},\bar{\sigma}_{22},\bar{\sigma}_{33},\mathbf{d}_{11},\mathbf{d}_{22},\mathbf{d}_{33},\bar{\sigma}^2_{23},\bar{\sigma}^2_{13},\bar{\sigma}^2_{12},\bar{\sigma}_{23}\bar{\sigma}_{13}\bar{\sigma}_{12},\mathbf{d}^2_{23},\mathbf{d}^2_{13},\mathbf{d}^2_{12},\mathbf{d}_{23}\mathbf{d}_{13}\mathbf{d}_{12},\bar{\sigma}_{23}\mathbf{d}_{23},\\ \bar{\sigma}_{13}\mathbf{d}_{13},\bar{\sigma}_{12}\mathbf{d}_{12},\mathbf{d}_{23}\bar{\sigma}_{13}\bar{\sigma}_{12},\mathbf{d}_{13}\bar{\sigma}_{12}\bar{\sigma}_{23},\mathbf{d}_{12}\bar{\sigma}_{23}\bar{\sigma}_{13},\bar{\sigma}_{23}\mathbf{d}_{13}\mathbf{d}_{12},\bar{\sigma}_{13}\mathbf{d}_{12}\mathbf{d}_{23},\bar{\sigma}_{12}\mathbf{d}_{23}\mathbf{d}_{13}\end{gathered} \tag{1}$$

where the normalized stress

$$\bar{\sigma}_{ij} = \frac{\sigma_{ij}}{\sigma_f} \tag{2}$$

where σ_f is the ultimate stress in a material principal direction, and the damage tensor $\mathbf{d}_{ij}$ is a symmetric tensor of the second rank (Talreja, 1994; Roy and Xu, 2001). One advantage of selecting this damage description is that the magnitude of the damage entity is typically less than one.

2.1. Special case

Consider a laminate with bi-axial microcracks oriented perpendicular to the X_1 and X_2 axis, subjected to inplane uniaxial loading in the X_1 direction under isothermal conditions as shown schematically in Fig. 1. Note that the axial cracks (i.e. cracks parallel to the X_1 axis) are assumed discontinuous in order to reflect realistic damage states in woven laminates subjected to uniaxial loading. For the special case of uniaxial loading, the states of stress and damage reduce to

$$\bar{\sigma}_{22} = \bar{\sigma}_{33} = \bar{\sigma}_{13} = \bar{\sigma}_{23} = \bar{\sigma}_{12} = 0$$

and

$$\mathbf{d}_{33} = \mathbf{d}_{13} = \mathbf{d}_{23} = \mathbf{d}_{12} = 0$$

Using the irreducible integrity bases from Eq. (1) and retaining terms up to second order in the normalized stress component $\bar{\sigma}_{11}$, and the two non-zero damage components $\mathbf{d}_{11}$ and $\mathbf{d}_{22}$, the Gibbs potential becomes,

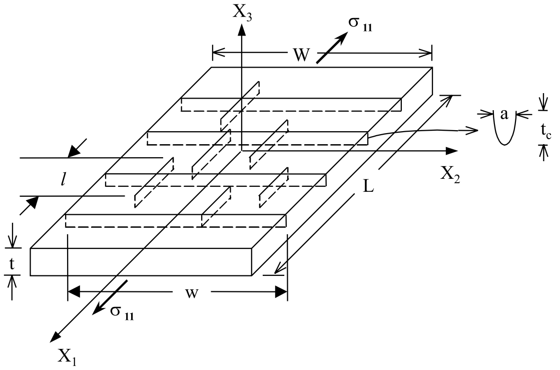

Fig. 1. Idealized schematic of a bi-axially micro-cracked laminate under uniaxial stress state.

$$\rho_s\phi = \hat{C}_0 + \hat{C}_1(\mathbf{d}_{11} + \mathbf{d}_{22}) + \hat{C}_2\mathbf{d}_{11}\mathbf{d}_{22} + \hat{C}_3(\mathbf{d}_{11}^2 + \mathbf{d}_{22}^2) + \hat{C}_4\overline{\sigma}_{11} + \hat{C}_5\overline{\sigma}_{11}\mathbf{d}_{11} + \hat{C}_6\overline{\sigma}_{11}\mathbf{d}_{22} + \hat{C}_7\overline{\sigma}_{11}^2 \tag{3}$$

where, ρ_s is the mass density of the laminate, and $\hat{C}_i$ are material coefficients independent of stress and damage, but may depend on concentration (m) and temperature (T). Eq. (3) was derived specifically for the case of a woven fabric laminate, and not for a monotape cross-ply laminate. It should be noted that Eq. (3) incorporates the special material symmetry condition in the plane of the laminate (X_1–X_2 plane) that is characteristic of a $[0/90/0/90]_s$ weave architecture, that is, two aligned woven laminas stacked on two identical woven laminas that have been flipped over about the central plane of the laminate. As a direct consequence of the weave architecture, orthogonal material symmetry exists for the in-plane directions, that is, for example, $E_{11} = E_{22}$ (refer to Fig. 1). Analogously, from a moisture diffusion standpoint, it can be argued that the through thickness diffusivity (D_3) is identically affected by moisture diffusing through cracks that are either parallel or perpendicular to the X_1 direction, in the absence of any applied stress. Therefore, the $\mathbf{d}_{11}$ and $\mathbf{d}_{22}$ terms should share the same coefficient in the Gibbs potential, as should the $(\mathbf{d}_{11})^2$ and $(\mathbf{d}_{22})^2$ terms. However, when applied stress (σ_{11}) is introduced, then this bi-axial symmetry is modified and the Gibbs potential must therefore include separate coefficients for the $\sigma_{11}\mathbf{d}_{11}$ and the $\sigma_{11}\mathbf{d}_{22}$ terms, as reflected in the use of C_5 and C_6.

The chemical potential of moisture in the polymer composite for this special case is defined as,

$$\begin{aligned}
\mu &= \rho_s\frac{\partial\phi}{\partial m} \\
&= \frac{\partial\hat{C}_0}{\partial m} + \frac{\partial\hat{C}_1}{\partial m}(\mathbf{d}_{11} + \mathbf{d}_{22}) + \hat{C}_1\left(\frac{\partial\mathbf{d}_{11}}{\partial m} + \frac{\partial\mathbf{d}_{22}}{\partial m}\right) + \frac{\partial\hat{C}_2}{\partial m}\mathbf{d}_{11}\mathbf{d}_{22} + \hat{C}_2\frac{\partial\mathbf{d}_{11}}{\partial m}\mathbf{d}_{22} + \hat{C}_2\frac{\partial\mathbf{d}_{22}}{\partial m}\mathbf{d}_{11} \\
&\quad + \frac{\partial\hat{C}_3}{\partial m}(\mathbf{d}_{11}^2 + \mathbf{d}_{22}^2) + \hat{C}_3\left(2\mathbf{d}_{11}\frac{\partial\mathbf{d}_{11}}{\partial m} + 2\mathbf{d}_{22}\frac{\partial\mathbf{d}_{22}}{\partial m}\right) + \frac{\partial\hat{C}_4}{\partial m}\overline{\sigma}_{11} + \hat{C}_4\frac{\partial\overline{\sigma}_{11}}{\partial m} + \frac{\partial\hat{C}_5}{\partial m}\overline{\sigma}_{11}\mathbf{d}_{11} + \hat{C}_5\overline{\sigma}_{11}\frac{\partial\mathbf{d}_{11}}{\partial m} \\
&\quad + \hat{C}_5\mathbf{d}_{11}\frac{\partial\overline{\sigma}_{11}}{\partial m} + \frac{\partial\hat{C}_6}{\partial m}\overline{\sigma}_{11}\mathbf{d}_{22} + \hat{C}_6\overline{\sigma}_{11}\frac{\partial\mathbf{d}_{22}}{\partial m} + \hat{C}_6\mathbf{d}_{22}\frac{\partial\overline{\sigma}_{11}}{\partial m} + \frac{\partial\hat{C}_7}{\partial m}\overline{\sigma}_{11}^2 + 2\hat{C}_7\overline{\sigma}_{11}\frac{\partial\overline{\sigma}_{11}}{\partial m}
\end{aligned} \tag{4}$$

Because chemical potential is, in this case, a function of σ_{11}, $\mathbf{d}_{11}$, $\mathbf{d}_{22}$, T, and m, hence,

$$\frac{\partial\mu}{\partial X_i} = \frac{\partial\mu}{\partial m}\frac{\partial m}{\partial X_i} + \frac{\partial\mu}{\partial T}\frac{\partial T}{\partial X_i} + \frac{\partial\mu}{\partial\overline{\sigma}_{11}}\frac{\partial\overline{\sigma}_{11}}{\partial X_i} + \frac{\partial\mu}{\partial\mathbf{d}_{11}}\frac{\partial\mathbf{d}_{11}}{\partial X_i} + \frac{\partial\mu}{\partial\mathbf{d}_{22}}\frac{\partial\mathbf{d}_{22}}{\partial X_i}$$

For the special case of uniform stress, damage, and temperature distributions, only the moisture concentration gradient term is dominant, giving the moisture flux term as,

$$D_i\frac{\partial\mu}{\partial X_i} = D_i\left(\frac{\partial\mu}{\partial m}\right)\left(\frac{\partial m}{\partial X_i}\right) = \overline{D}_i\left(\frac{\partial m}{\partial X_i}\right) \tag{5}$$

where

$$\overline{D}_i = D_i\left(\frac{\partial\mu}{\partial m}\right)$$

In Eq. (5), D_i are the components of diffusivity in the material principal directions, and $\overline{D}_i$ are the components of *effective* diffusivity in the material principal directions. Note that repeated indices do not imply summation in Eq. (5). Substitute Eq. (4) into Eq. (5) gives,

$$
\begin{aligned}
D_i \frac{\partial \mu}{\partial X_i} &= D_i \left(\frac{\partial \mu}{\partial m} \right) \left(\frac{\partial m}{\partial X_i} \right) \\
&= D_i \left[\frac{\partial^2 \hat{C}_0}{\partial m^2} . + \frac{\partial^2 \hat{C}_1}{\partial m^2} (\mathbf{d}_{11} + \mathbf{d}_{22}) + 2 \frac{\partial \hat{C}_1}{\partial m} \left(\frac{\partial \mathbf{d}_{11}}{\partial m} + \frac{\partial \mathbf{d}_{22}}{\partial m} \right) + \hat{C}_1 \left(\frac{\partial^2 \mathbf{d}_{11}}{\partial m^2} + \frac{\partial^2 \mathbf{d}_{22}}{\partial m^2} \right) + \frac{\partial^2 \hat{C}_2}{\partial m^2} \mathbf{d}_{11} \mathbf{d}_{22} \right. \\
&\quad + 2 \frac{\partial \hat{C}_2}{\partial m} \frac{\partial \mathbf{d}_{11}}{\partial m} \mathbf{d}_{22} + 2 \frac{\partial \hat{C}_2}{\partial m} \frac{\partial \mathbf{d}_{22}}{\partial m} \mathbf{d}_{11} + \hat{C}_2 \frac{\partial^2 \mathbf{d}_{11}}{\partial m^2} \mathbf{d}_{22} + 2 \hat{C}_2 \frac{\partial \mathbf{d}_{11}}{\partial m} \frac{\partial \mathbf{d}_{22}}{\partial m} + \hat{C}_2 \frac{\partial^2 \mathbf{d}_{22}}{\partial m^2} \mathbf{d}_{11} + \frac{\partial^2 \hat{C}_3}{\partial m^2} (\mathbf{d}_{11}^2 + \mathbf{d}_{22}^2) \\
&\quad + 4 \frac{\partial \hat{C}_3}{\partial m} \left(\mathbf{d}_{11} \frac{\partial \mathbf{d}_{11}}{\partial m} + \mathbf{d}_{22} \frac{\partial \mathbf{d}_{22}}{\partial m} \right) + 2 \hat{C}_3 \left(\frac{\partial \mathbf{d}_{11}}{\partial m} \frac{\partial \mathbf{d}_{11}}{\partial m} + \mathbf{d}_{11} \frac{\partial^2 \mathbf{d}_{11}}{\partial m^2} + \frac{\partial \mathbf{d}_{22}}{\partial m} \frac{\partial \mathbf{d}_{22}}{\partial m} + \mathbf{d}_{22} \frac{\partial^2 \mathbf{d}_{22}}{\partial m^2} \right) \\
&\quad + \frac{\partial^2 \hat{C}_4}{\partial m^2} \overline{\sigma}_{11} + 2 \frac{\partial \hat{C}_4}{\partial m} \frac{\partial \overline{\sigma}_{11}}{\partial m} + \hat{C}_4 \frac{\partial^2 \overline{\sigma}_{11}}{\partial m^2} + \frac{\partial^2 \hat{C}_5}{\partial m^2} \overline{\sigma}_{11} \mathbf{d}_{11} + 2 \frac{\partial \hat{C}_5}{\partial m} \frac{\partial \overline{\sigma}_{11}}{\partial m} \mathbf{d}_{11} + 2 \frac{\partial \hat{C}_5}{\partial m} \frac{\partial \mathbf{d}_{11}}{\partial m} \overline{\sigma}_{11} \\
&\quad + 2 \hat{C}_5 \frac{\partial \overline{\sigma}_{11}}{\partial m} \frac{\partial \mathbf{d}_{11}}{\partial m} + \hat{C}_5 \overline{\sigma}_{11} \frac{\partial^2 \mathbf{d}_{11}}{\partial m^2} + \hat{C}_5 \mathbf{d}_{11} \frac{\partial^2 \overline{\sigma}_{11}}{\partial m^2} + \frac{\partial^2 \hat{C}_6}{\partial m^2} \overline{\sigma}_{11} \mathbf{d}_{22} + 2 \frac{\partial \hat{C}_6}{\partial m} \frac{\partial \overline{\sigma}_{11}}{\partial m} \mathbf{d}_{22} \\
&\quad + 2 \frac{\partial \hat{C}_6}{\partial m} \frac{\partial \mathbf{d}_{22}}{\partial m} \overline{\sigma}_{11} + 2 \hat{C}_6 \frac{\partial \overline{\sigma}_{11}}{\partial m} \frac{\partial \mathbf{d}_{22}}{\partial m} + \hat{C}_6 \overline{\sigma}_{11} \frac{\partial^2 \mathbf{d}_{22}}{\partial m^2} + \hat{C}_6 \mathbf{d}_{22} \frac{\partial^2 \overline{\sigma}_{11}}{\partial m^2} + \frac{\partial^2 \hat{C}_7}{\partial m^2} \overline{\sigma}_{11}^2 \\
&\quad \left. + 4 \frac{\partial \hat{C}_7}{\partial m} \frac{\partial \overline{\sigma}_{11}}{\partial m} \overline{\sigma}_{11} + 2 \hat{C}_7 \frac{\partial \overline{\sigma}_{11}}{\partial m} \frac{\partial \overline{\sigma}_{11}}{\partial m} + 2 \hat{C}_7 \overline{\sigma}_{11} \frac{\partial^2 \overline{\sigma}_{11}}{\partial m^2} \right] \left(\frac{\partial m}{\partial X_i} \right) (6)
\end{aligned}
$$

For the special external stress-free case where $\overline{\sigma}_{11} = 0$, Eq. (6) reduces to,

$$
\begin{aligned}
D_i \frac{\partial \mu}{\partial X_i} &= D_i \left[\frac{\partial^2 \hat{C}_0}{\partial m^2} + \frac{\partial^2 \hat{C}_1}{\partial m^2} (\mathbf{d}_{11} + \mathbf{d}_{22}) + 2 \frac{\partial \hat{C}_1}{\partial m} \left(\frac{\partial \mathbf{d}_{11}}{\partial m} + \frac{\partial \mathbf{d}_{22}}{\partial m} \right) + \hat{C}_1 \left(\frac{\partial^2 \mathbf{d}_{11}}{\partial m^2} + \frac{\partial^2 \mathbf{d}_{22}}{\partial m^2} \right) + \frac{\partial^2 \hat{C}_2}{\partial m^2} \mathbf{d}_{11} \mathbf{d}_{22} \right. \\
&\quad + 2 \frac{\partial \hat{C}_2}{\partial m} \frac{\partial \mathbf{d}_{11}}{\partial m} \mathbf{d}_{22} + 2 \frac{\partial \hat{C}_2}{\partial m} \frac{\partial \mathbf{d}_{22}}{\partial m} \mathbf{d}_{11} + \hat{C}_2 \frac{\partial^2 \mathbf{d}_{11}}{\partial m^2} \mathbf{d}_{22} + 2 \hat{C}_2 \frac{\partial \mathbf{d}_{11}}{\partial m} \frac{\partial \mathbf{d}_{22}}{\partial m} + \hat{C}_2 \frac{\partial^2 \mathbf{d}_{22}}{\partial m^2} \mathbf{d}_{11} + \frac{\partial^2 \hat{C}_3}{\partial m^2} (\mathbf{d}_{11}^2 + \mathbf{d}_{22}^2) \\
&\quad \left. + 4 \frac{\partial \hat{C}_3}{\partial m} \left(\mathbf{d}_{11} \frac{\partial \mathbf{d}_{11}}{\partial m} + \mathbf{d}_{22} \frac{\partial \mathbf{d}_{22}}{\partial m} \right) + 2 \hat{C}_3 \left(\frac{\partial \mathbf{d}_{11}}{\partial m} \frac{\partial \mathbf{d}_{11}}{\partial m} + \mathbf{d}_{11} \frac{\partial^2 \mathbf{d}_{11}}{\partial m^2} + \frac{\partial \mathbf{d}_{22}}{\partial m} \frac{\partial \mathbf{d}_{22}}{\partial m} + \mathbf{d}_{22} \frac{\partial^2 \mathbf{d}_{22}}{\partial m^2} \right) \right] \left(\frac{\partial m}{\partial X_i} \right)
\end{aligned}
\tag{7}
$$

Based on a definition of a damage entity originally proposed by Talreja (1994), it can be shown that the *pre-existing* non-zero damage components $\mathbf{d}_{11}$, $\mathbf{d}_{22}$ are given by,

$$
\begin{aligned}
\mathbf{d}_{11} &= \frac{\kappa(m, T) t_c^2 \delta_1}{t} \\
\mathbf{d}_{22} &= \frac{\kappa(m, T) t_c^2 \delta_2}{t}
\end{aligned}
\tag{8}
$$

where $\kappa(m, T)$ is an experimentally determined influence parameter on crack opening displacement, t_c is the crack size as shown in Fig. 1, t is the total thickness of the laminate, and δ_1, δ_2 are crack densities in laminate longitudinal (X_1) and transverse (X_2) directions respectively. In the definition of the Gibbs potential, it is assumed that damage and stress are the two independent state variables in the formulation. In addition, the focus of this paper is on the influence of pre-existing damage on the diffusion characteristics of the laminate, that is, the micro-cracks have been generated by load application prior to the diffusion

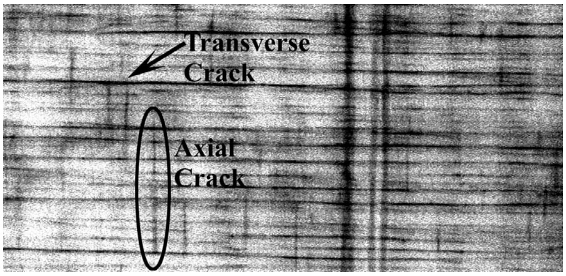

Fig. 2. Radiograph from a specimen containing fatigue induced bi-axial cracks.

experiments. When the applied load is removed it is assumed that the micro-cracks still remain sufficiently open, as quantified by $\kappa(m, T)t_c$, to allow ingress of water vapor into the cracks and perhaps even liquid water through capillary action. It should be noted that $\kappa(m, T)$ is defined to depend only on the moisture concentration and the ambient temperature but not on stress. The diffusion enhancing effect of applied tensile stress in the presence of pre-existing damage is included in the model through the damage-stress interaction terms in the Gibbs potential given by $C_5\sigma_{11}\mathbf{d}_{11}$ and $C_6\sigma_{11}\mathbf{d}_{22}$.

Subsequent to the moisture uptake experiments, penetrant enhanced radiography was employed to assess the damage-state in the composite laminates. An example of a section taken from such a radiograph is shown in Fig. 2 for a specimen that was subjected to 75,000 cycles of uniaxial loading ($R = 0.1$, $f = 10$ Hz) at 521 MPa (75.6 ksi, 70% UTS). We note that while some interbundle separation (commonly referred to as a meta-delamination) occurs, delamination damage mode is not incorporated into the present diffusion model because the influence of meta-delaminations on laminate through-thickness diffusion is deemed insignificant. As may be observed from the radiograph shown in Fig. 2, the longitudinal cracks do not extend the full length of the laminate in uniaxial fatigue of AS4/PR500 woven composite, where as the transverse cracks span the entire width. Consequently, for the longitudinal cracks, the crack density is calculated as,

$$\delta_1 = \frac{\sum_{i=1}^{M} l_i}{WL}$$

where M is the number of longitudinal cracks each having a length of l_i within a specimen volume of WLt.

The transverse crack density is calculated as

$$\delta_2 = \frac{\sum_{i=1}^{N} w_i}{WL}$$

where, N is the number of transverse cracks, and w is the length of the ith transverse crack. For transverse cracks, the crack length is equal to the specimen width W, so that we have

$$\delta_2 = \frac{N}{L}$$

If it is assumed that swelling due to moisture absorption influences only the opening displacement without significantly affecting either the crack size, t_c, or the crack density, δ_1, δ_2, then,

$$\begin{aligned}\frac{\partial \mathbf{d}_{11}}{\partial m} &= \frac{t_c^2\delta_1}{t}\frac{\partial \kappa}{\partial m}\\ \frac{\partial^2 \mathbf{d}_{11}}{\partial m^2} &= \frac{t_c^2\delta_1}{t}\frac{\partial^2 \kappa}{\partial m^2}\\ \frac{\partial \mathbf{d}_{22}}{\partial m} &= \frac{t_c^2\delta_2}{t}\frac{\partial \kappa}{\partial m}\\ \frac{\partial^2 \mathbf{d}_{22}}{\partial m^2} &= \frac{t_c^2\delta_2}{t}\frac{\partial^2 \kappa}{\partial m^2}\end{aligned} \tag{9}$$

Taking the definitions of damage and its derivative given respectively by Eqs. (8) and (9) and substituting in Eq. (7) results in an expression for moisture flux in terms of an effective diffusivity and concentration gradient as indicated on the right-hand side of Eq. (10),

$$D_i\frac{\partial \mu}{\partial X_i} = \overline{D}_i\frac{\partial m}{\partial X_i} \tag{10}$$

where, each orthotropic component of effective diffusivity ($\overline{D}_i$) can be obtained as a quadratic function of the crack density given by,

$$\begin{aligned}\overline{D}_i &= D_i\frac{\partial \mu}{\partial m}\\ &= D_i\left\{\frac{\partial^2\hat{C}_0}{\partial m^2} + \left(\kappa\frac{\partial^2\hat{C}_1}{\partial m^2} + 2\frac{\partial\hat{C}_1}{\partial m}\frac{\partial\kappa}{\partial m} + \hat{C}_1\frac{\partial^2\kappa}{\partial m^2}\right)\frac{t_c^2}{t}(\delta_1+\delta_2) + \left[\frac{\partial^2\hat{C}_2}{\partial m^2}\kappa^2 + 4\kappa\frac{\partial\hat{C}_2}{\partial m}\frac{\partial\kappa}{\partial m}\right.\right.\\ &\qquad \left. + 2\kappa\hat{C}_2\frac{\partial^2\kappa}{\partial m^2} + 2\hat{C}_2\left(\frac{\partial\kappa}{\partial m}\right)^2\right]\left(\frac{t_c^2}{t}\right)^2\delta_1\delta_2 + \left[\frac{\partial^2\hat{C}_3}{\partial m^2}\kappa^2 + 4\kappa\frac{\partial\hat{C}_3}{\partial m}\frac{\partial\kappa}{\partial m} + 2\kappa\hat{C}_3\frac{\partial^2\kappa}{\partial m^2}\right.\\ &\qquad \left.\left. + 2\hat{C}_3\left(\frac{\partial\kappa}{\partial m}\right)^2\right]\left(\frac{t_c^2}{t}\right)^2(\delta_1^2+\delta_2^2)\right\}\end{aligned} \tag{11}$$

Arranging terms in Eq. (11) yields,

$$\overline{D}_i = C_0 + C_1(\delta_1+\delta_2) + C_2\delta_1\delta_2 + C_3(\delta_1^2+\delta_1^2) \tag{12}$$

where,

$$C_0(m,T) = D_i\frac{\partial^2\hat{C}_0}{\partial m^2} \tag{13}$$

$$C_1(m,T) = D_i\left(\kappa\frac{\partial^2\hat{C}_1}{\partial m^2} + 2\frac{\partial\hat{C}_1}{\partial m}\frac{\partial\kappa}{\partial m} + \hat{C}_1\frac{\partial^2\kappa}{\partial m^2}\right)\frac{t_c^2}{t} \tag{14}$$

$$C_2(m,T) = D_i\left[\frac{\partial^2\hat{C}_2}{\partial m^2}\kappa^2 + 4\kappa\frac{\partial\hat{C}_2}{\partial m}\frac{\partial\kappa}{\partial m} + 2\kappa\hat{C}_2\frac{\partial^2\kappa}{\partial m^2} + 2\hat{C}_2\left(\frac{\partial\kappa}{\partial m}\right)^2\right]\left(\frac{t_c^2}{t}\right)^2 \tag{15}$$

$$C_3(m,T) = D_i\left[\frac{\partial^2\hat{C}_3}{\partial m^2}\kappa^2 + 4\kappa\frac{\partial\hat{C}_3}{\partial m}\frac{\partial\kappa}{\partial m} + 2\kappa\hat{C}_3\frac{\partial^2\kappa}{\partial m^2} + 2\hat{C}_3\left(\frac{\partial\kappa}{\partial m}\right)^2\right]\left(\frac{t_c^2}{t}\right)^2 \tag{16}$$

Conservation of diffusing mass of penetrant within a unit volume of the polymer requires,

$$\frac{\partial m}{\partial t} = -\frac{\partial f_i}{\partial X_i} \tag{17}$$

where, in the absence of temperature, stress and damage gradients, moisture flux f_i for orthotropic symmetry is assumed to be of the form,

$$f_i = -D_i \frac{\partial \mu}{\partial X_i} \tag{18}$$

where D_i are the diffusion coefficients in material principal directions. Note that while repeated indices imply summation in Eq. (18), summation is not implied in Eq. (17). Combining Eqs. (17) and (18), gives the governing equation for diffusion in an orthotropic medium,

$$\frac{\partial m}{\partial t} = \frac{\partial}{\partial X_i}\left(D_i \frac{\partial \mu}{\partial X_i}\right) \tag{19}$$

Repeated indices imply summation in Eq. (19), with $i = 1, 2, 3$ for three-dimensional diffusion. Substituting Eqs. (10) and (12) in Eq. (19) yields the governing equation for moisture diffusion in an unloaded orthotropic laminate with uniform damage in a volume-average sense,

$$\frac{\partial m}{\partial t} = \frac{\partial}{\partial X_i}\left\{\left[C_0 + C_1(\delta_1 + \delta_2) + C_2\delta_1\delta_2 + C_3\left(\delta_1^2 + \delta_2^2\right)\right]\frac{\partial m}{\partial X_i}\right\} \tag{20}$$

For modeling absorption and/or desorption in a damaged laminate in the through-thickness, i.e., in the X_3 direction, Eq. (20) reduces to

$$\frac{\partial m}{\partial t} = \frac{\partial}{\partial X_3}\left\{\left[C_0 + C_1(\delta_1 + \delta_2) + C_2\delta_1\delta_2 + C_3\left(\delta_1^2 + \delta_2^2\right)\right]\frac{\partial m}{\partial X_3}\right\} \tag{21}$$

3. Boundary condition and maximum saturation level

For a linear elastic composite laminate, the chemical potential of the ambient vapor μ_b on the boundary is a constant with respect to time, i.e.,

$$\mu\left(m, T, \mathbf{d}_{ij}\right) = \mu_b = \text{constant on boundary} \tag{22}$$

Assuming negligible change in stress and damage with moisture concentration, Eq. (4) reduces to,

$$\begin{aligned}\mu\left(m, T, \mathbf{d}_{ij}\right) &= \frac{\partial \hat{C}_0}{\partial m} + \frac{\partial \hat{C}_1}{\partial m}(\mathbf{d}_{11} + \mathbf{d}_{22}) + \frac{\partial \hat{C}_2}{\partial m}\mathbf{d}_{11}\mathbf{d}_{22} + \frac{\partial \hat{C}_3}{\partial m}(\mathbf{d}_{11}^2 + \mathbf{d}_{22}^2) \\ &= A_0(m, T) + A_1(m, T)(\mathbf{d}_{11} + \mathbf{d}_{22}) + A_2(m, T)\mathbf{d}_{11}\mathbf{d}_{22} + A_3(m, T)(\mathbf{d}_{11}^2 + \mathbf{d}_{22}^2)\end{aligned} \tag{23}$$

Assuming that moisture concentration $m \ll 1$ as is typically the case for a PMC, and expanding the coefficients in Eq. (23) in powers of m and retaining only first-order terms in m yields,

$$\begin{aligned}\mu\left(m, T, \mathbf{d}_{ij}\right) = {}& \left\lfloor \overline{A}_0(T) + \hat{A}_0(T)m \right\rfloor + \left\lfloor \overline{A}_1(T) + \hat{A}_1(T)m \right\rfloor(\mathbf{d}_{11} + \mathbf{d}_{22}) + \left[\overline{A}_2(T) + \hat{A}_2(T)m\right]\mathbf{d}_{11}\mathbf{d}_{22} \\ & + \left[\overline{A}_3(T) + \hat{A}_3(T)m\right](\mathbf{d}_{11}^2 + \mathbf{d}_{22}^2)\end{aligned} \tag{24}$$

Combining Eqs. (22) and (24) gives concentration on the boundary (m_b) as a function of damage,

$$m_b = \frac{\mu_b - \overline{A}_0(T) - \overline{A}_1(T)(\mathbf{d}_{11} + \mathbf{d}_{22}) - \overline{A}_2(T)\mathbf{d}_{11}\mathbf{d}_{22} - \overline{A}_3(T)(\mathbf{d}_{11}^2 + \mathbf{d}_{22}^2)}{\hat{A}_0(T) + \hat{A}_1(T)(\mathbf{d}_{11} + \mathbf{d}_{22}) + \hat{A}_2(T)\mathbf{d}_{11}\mathbf{d}_{22} + \hat{A}_3(T)(\mathbf{d}_{11}^2 + \mathbf{d}_{22}^2)} \tag{25}$$

Dividing numerator and denominator in Eq. (25) by $\hat{A}_0(T)$,

$$m_\mathrm{b} = \frac{\hat{a}_0(T) + \hat{a}_1(T)(\mathbf{d}_{11} + \mathbf{d}_{22}) + \hat{a}_2(T)\mathbf{d}_{11}\mathbf{d}_{22} + \hat{a}_3(T)(\mathbf{d}_{11}^2 + \mathbf{d}_{22}^2)}{1 + \hat{a}_4(T)(\mathbf{d}_{11} + \mathbf{d}_{22}) + \hat{a}_5(T)\mathbf{d}_{11}\mathbf{d}_{22} + \hat{a}_6(T)(\mathbf{d}_{11}^2 + \mathbf{d}_{22}^2)} \tag{26}$$

where,

$$\hat{a}_0(T) = \frac{\mu_\mathrm{b} - \overline{A}_0(T)}{\hat{A}_0(T)}$$

$$\hat{a}_1(T) = \frac{\overline{A}_1(T)}{\hat{A}_0(T)}$$

and so on.

In the interest of solution tractability if it is assumed that $\mathbf{d}_{11}, \mathbf{d}_{22} \ll 1$, then we may ignore the damage terms beyond first order in the numerator and denominator of Eq. (26), giving,

$$m_\mathrm{b} = \frac{\hat{a}_0(T) + \hat{a}_1(T)(\mathbf{d}_{11} + \mathbf{d}_{22})}{1 + \hat{a}_4(T)(\mathbf{d}_{11} + \mathbf{d}_{22})} \tag{27}$$

Expanding Eq. (27) in terms of $(\mathbf{d}_{11} + \mathbf{d}_{22})$ using Taylor series and retaining terms up to second order provides an approximate expression for the concentration on the boundary in terms of bi-axial damage state,

$$m_\mathrm{b} = \overline{a}_0(T) + \overline{a}_1(T)(\mathbf{d}_{11} + \mathbf{d}_{22}) + \overline{a}_2(T)(\mathbf{d}_{11} + \mathbf{d}_{22})^2 \tag{28}$$

where,

$$\overline{a}_0(T) = \hat{a}_0(T)$$

$$\overline{a}_1(T) = \hat{a}_1(T) - \hat{a}_0(T)\hat{a}_4(T)$$

$$\overline{a}_2(T) = \hat{a}_4(T)[\hat{a}_0(T)\hat{a}_4(T) - \hat{a}_1(T)]$$

Recalling from Eq. (8),

$$\mathbf{d}_{11} = \frac{\kappa(m,T)t_\mathrm{c}^2\delta_1}{t}, \quad \mathbf{d}_{22} = \frac{\kappa(m,T)t_\mathrm{c}^2\delta_2}{t},$$

and substituting in Eq. (28), the boundary moisture concentration given in Eq. (28) can now be expressed in terms of bi-axial crack densities as,

$$m_\mathrm{b} = a_0(T) + a_1(m,T)(\delta_1 + \delta_2) + a_2(m,T)(\delta_1 + \delta_2)^2 \tag{29}$$

where, a_0, a_1, and a_2 are constants associated with the moisture concentration level and temperature and are given by,

$$a_0(T) = \overline{a}_0(T)$$

$$a_1(m,T) = \overline{a}_1(T)\left\{\frac{\kappa(m,T)t_\mathrm{c}^2}{t}\right\}$$

$$a_2(m,T) = \overline{a}_2(T)\left\{\frac{\kappa(m,T)t_\mathrm{c}^2}{t}\right\}^2$$

Finally, the maximum moisture content in the specimen at saturation can then be obtained as,

$$M_m = m_b(\text{volume of specimen}) \tag{30}$$

4. Closed form solution for diffusion through laminate thickness

If the crack-densities are uniform in a volume-averaged sense, the diffusion governing equation given by Eq. (21) is amenable to a closed form solution subject to the boundary condition defined by Eq. (29). The resulting through-thickness, time-varying moisture concentration profile in terms of bi-axial crack densities is given by,

$$m_t = \left[a_0(T) + a_1(m,T)(\delta_1+\delta_2) + a_2(m,T)(\delta_1+\delta_2)^2\right]\left\{1 - \frac{4}{\pi}\sum_{n=0}^{\infty}\frac{(-1)^n}{(2n+1)}\exp\left[-(2n+1)^2\left(\frac{\pi}{h}\right)^2\left[C_0 + C_1(\delta_1+\delta_2) + C_2\delta_1\delta_2 + C_3(\delta_1^2+\delta_2^2)\right]t\right]\cos\frac{(2n+1)\pi x}{h}\right\} \tag{31}$$

where, h is laminate thickness and t is time. Integrating Eq. (31) over the laminate thickness results in an expression for the total moisture uptake per unit area of the laminate surface as a function of bi-axial crack densities,

$$M_t = \left[a_0(T) + a_1(m,T)(\delta_1+\delta_2) + a_2(m,T)(\delta_1+\delta_2)^2\right]\left\{1 - \frac{8}{\pi^2}\sum_{n=0}^{\infty}\frac{1}{(2n+1)^2}\exp\left[-(2n+1)^2\left(\frac{\pi}{h}\right)^2\left[C_0 + C_1(\delta_1+\delta_2) + C_2\delta_1\delta_2 + C_3(\delta_1^2+\delta_2^2)\right]t\right]\right\} \tag{32}$$

5. Hygrothermal testing and diffusion data characterization

In order to characterize the damage-diffusivity influence coefficients C_0, C_1, C_2, C_3 and the damage-saturation influence coefficients a_0, a_1, a_2, moisture weight gain data for graphite/epoxy 5-harness satin $[0/90/0/90]_s$ laminate with different bi-axial micro-crack densities were obtained from hygrothermal tests performed at Virginia Polytechnic Institute and State University. Specifically, test specimens were mechanically pre-cracked by uniaxial fatigue or by static loading and then fully immersed in water at 65°C. The bi-axial micro-crack densities in terms of cracks/cm for the specimens are listed in Table 1 together with the type of loading that was used for pre-cracking the specimen. A set of uncracked specimens was also included in the test matrix as a control set. The specimens were not subjected to any applied mechanical stress during moisture absorption. The last two columns of Table 1 list the diffusivity and maximum moisture weight gain (%) measured for each specimen type from test data. Fig. 3 shows the moisture weight

Table 1
Diffusivity and maximum moisture uptake obtained from hygrothermal tests performed at different damage levels

Specimen	Load type	δ_1 (cm^{-1})	δ_2 (cm^{-1})	D (cm^2/s)	M_m (%)
1	No damage	0	0	8.621E – 09	0.40808
2	21.4 KN (static)	0	7.35	1.265E – 08	0.45255
3	100,000 cycles	1.44	24.7	5.341E – 08	0.50715
4	200,000 cycles	4.95	25.2	1.936E – 07	0.60336
5	300,000 cycles	1.71	25.2	9.634E – 08	0.55616

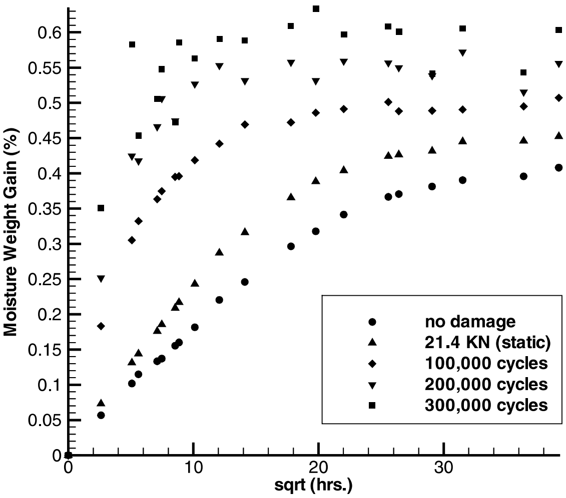

Fig. 3. Moisture uptake test data for specimens 1–5.

gain (%) vs. square root of time data for the five test specimens. The damage–diffusivity influence coefficients C_0, C_1, C_2, C_3 and the damage-saturation influence coefficients a_0, a_1, a_2 for each test specimen were extracted from weight gain data using a simple quadratic least-squares curve-fit procedure outlined below. It should be noted that test data from only the first four specimens (i.e., specimens 1–4) were employed to characterize the influence coefficients. The fifth data set (specimen 5) was held in reserve for verification of model prediction.

6. Least-squares curve-fit procedure

Let

$$D(\delta_1^k, \delta_2^k) = C_0 + C_1(\delta_1^k + \delta_2^k) + C_2\delta_1^k\delta_2^k + C_3\left(\delta_1^{k^2} + \delta_2^{k^2}\right) \tag{33}$$

and

$$E = \sum_{k=1}^{N}\left[D_k - D(\delta_1^k, \delta_2^k)\right]^2 \tag{34}$$

where, E is least square error, N is the number of test data points, D_k is the kth test data point, δ_1^k is the crack density in laminate 1-direction corresponding to kth data point, δ_2^k is the crack density in laminate 2-direction corresponding to kth data point.

The variation of the least square error should be zero, that is,

$$\delta E = \sum_{k=1}^{N}(D_k - D)\delta D = 0 \tag{35}$$

Substituting Eq. (12) into Eq. (35) gives,

$$\sum_{k=1}^{N}(D_k - D)\left[\delta C_0 + \delta C_1(\delta_1^k + \delta_2^k) + \delta C_2\delta_1^k\delta_2^k + \delta C_3\left(\delta_1^{k^2} + \delta_2^{k^2}\right)\right] = 0 \tag{36}$$

Since all δC_i are arbitrary variations, the coefficients of δC_i must be zero, giving four Eqs. (37)–(40) that can be solved for the four influence coefficients C_0, C_1, C_2, C_3,

$$NC_0 + \left[\sum_{k=1}^{N}\left(\delta_1^k + \delta_2^k\right)\right]C_1 + \left[\sum_{k=1}^{N}\left(\delta_1^k\delta_2^k\right)\right]C_2 + \left[\sum_{k=1}^{N}\left(\delta_1^{k2} + \delta_2^{k2}\right)\right]C_3 = \sum_{k=1}^{N}D_k \tag{37}$$

$$\begin{aligned}&\left[\sum_{k=1}^{N}\left(\delta_1^k + \delta_2^k\right)\right]C_0 + \left[\sum_{k=1}^{N}\left(\delta_1^k + \delta_2^k\right)^2\right]C_1 + \left[\sum_{k=1}^{N}\left(\delta_1^k + \delta_2^k\right)\left(\delta_1^k\delta_2^k\right)\right]C_2 \\ &\quad + \left[\sum_{k=1}^{N}\left(\delta_1^k + \delta_2^k\right)\left(\delta_1^{k2} + \delta_2^{k2}\right)\right]C_3 = \sum_{k=1}^{N}D_k\left(\delta_1^k + \delta_2^k\right)\end{aligned} \tag{38}$$

$$\begin{aligned}&\left[\sum_{k=1}^{N}\left(\delta_1^k\delta_2^k\right)\right]C_0 + \left[\sum_{k=1}^{N}\left(\delta_1^k + \delta_2^k\right)\left(\delta_1^k\delta_2^k\right)\right]C_1 + \left[\sum_{k=1}^{N}\left(\delta_1^k\delta_2^k\right)^2\right]C_2 + \left[\sum_{k=1}^{N}\left(\delta_1^{k2} + \delta_2^{k2}\right)\left(\delta_1^k\delta_2^k\right)\right]C_3 \\ &\quad = \sum_{k=1}^{N}D_k\left(\delta_1^k\delta_2^k\right)\end{aligned} \tag{39}$$

$$\begin{aligned}&\left[\sum_{k=1}^{N}\left(\delta_1^{k2} + \delta_2^{k2}\right)\right]C_0 + \left[\sum_{k=1}^{N}\left(\delta_1^k + \delta_2^k\right)\left(\delta_1^{k2} + \delta_2^{k2}\right)\right]C_1 + \left[\sum_{k=1}^{N}\left(\delta_1^k\delta_2^k\right)\left(\delta_1^{k2} + \delta_2^{k2}\right)\right]C_2 \\ &\quad + \left[\sum_{k=1}^{N}\left(\delta_1^{k2} + \delta_2^{k2}\right)^2\right]C_3 = \sum_{k=1}^{N}D_k\left(\delta_1^{k2} + \delta_2^{k2}\right)\end{aligned} \tag{40}$$

A similar procedure was employed to obtain the three damage-saturation influence coefficients a_0, a_1, a_2 and is not presented separately here. The characterized values of the influence coefficients are listed in Tables 2 and 3, respectively. Upon characterization, these coefficients were then used to calculate the effective diffusivity given by Eq. (12), and the maximum saturation level given by Eqs. (29) and (30). The values of diffusivity and maximum saturation level for the first four test specimens were computed by employing the influence coefficients from Tables 2 and 3 in the proposed model and are listed in Table 4. As can be expected, a comparison of the calculated results presented in Table 4 with the test data in Table 1 reveals that the values calculated using the model agree closely with the original test data. While this constitutes a necessary check, it does not conclusively validate the model because the same set of test data

Table 2
Damage-diffusivity influence coefficients characterized using specimens 1–4

C_0 (cm^2/s)	0.86210E − 08
C_1 (cm^3/s)	0.98573E − 09
C_2 (cm^4/s)	0.15594E − 08
C_3 (cm^4/s)	−0.59533E − 10

Table 3
Damage-saturation influence coefficients characterized using specimens 1–4

a_0 (g)	0.41959E + 00
a_1 (g cm)	0.41541E − 03
a_2 (g cm^2)	0.16178E − 03

Table 4
Diffusivity and maximum moisture uptake obtained by using the proposed model at various damage levels for specimens 1–4

Specimen	δ_1 (cm^{-1})	δ_2 (cm^{-1})	D (cm^2/s)	M_m (%)
1	0	0	8.6210E − 09	0.41959
2	0	7.35	1.2653E − 08	0.43138
3	1.44	24.7	5.3409E − 08	0.50499
4	4.95	25.2	1.9306E − 07	0.57918

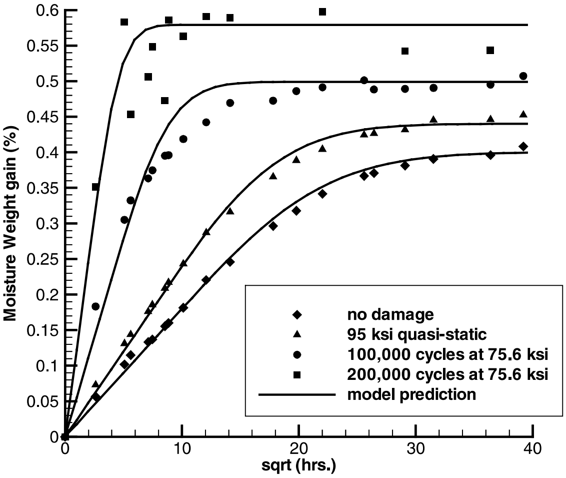

Fig. 4. Moisture uptake test data for specimens 1–4 for comparison with model prediction.

was used to obtain the influence coefficients. The four solid lines in Fig. 4 are model results for moisture uptake obtained using Eq. (32) and they merely serve to verify the accuracy of the influence coefficient characterization procedure for specimens 1–4.

7. Model verification

For actual model verification, Eq. (32) was applied to simulate the moisture uptake in test specimen 5, that was not included in the influence coefficient characterization data set. The influence coefficients listed in Tables 2 and 3 were used for this purpose, in conjunction with crack densities of $\delta_1 = 1.71$ and $\delta_2 = 25.2$ cracks/cm listed in Table 1 for specimen 5. The solid line in Fig. 5 shows predicted moisture weight gain as a function of time. The solid circles depict test data. Despite the scatter in the test data, the agreement between the test data and model prediction is deemed reasonable. The laminate diffusivity and maximum saturation level predicted by the model for this case are listed in Table 5 together with test data for comparison. While there is a 33% error in predicted diffusivity, the error in the predicted maximum saturation level is less than 2%. It is likely that the accuracy of the diffusivity prediction can be greatly improved through the collection of more data points during the early stages of each experiment.

These results seem to confirm that retaining only up to the quadratic terms in damage in the expansion of the Gibbs potential is a valid modeling approximation for the material system under consideration. More model verification tests are necessary to fully validate the hypothesis.

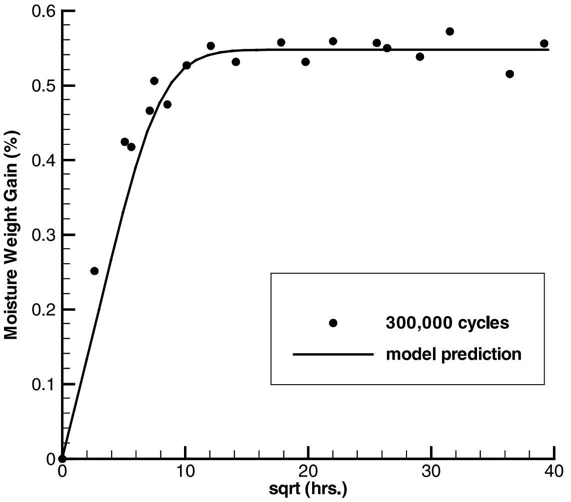

Fig. 5. Moisture uptake test data for specimen 5 and comparison with model prediction.

Table 5
Prediction of diffusivity and maximum saturation level for crack density $\delta_1 = 1.71$ and $\delta_2 = 25.2$ cracks/cm using proposed model

	Diffusivity (cm^2/s)	% Error in D	M_m (%)	% Error in M_m
Model prediction	6.437E − 08	33.2	0.54792	1.5
Test data	9.634E − 08	–	0.55616	–

8. Discussion and conclusions

A modeling methodology based on irreversible thermodynamics developed within the framework of composite macro-mechanics was presented to allow characterization of anomalous (non-Fickian) diffusion coefficients from moisture weight gain data for laminated composites with bi-axial damage. A symmetric damage tensor based on continuum damage mechanics was incorporated in this model by invoking the principle of invariance with respect to coordinate transformations. To maintain tractability, the diffusion governing equations were simplified for the special case of a laminate with uniform matrix cracks that is subjected to a uniaxial tensile stress state. Because of the macro-mechanics formulation employed in developing this model, the model is currently restricted to the study of global laminate absorption/desorption characteristics in the presence of non-evolving damage states. An alternative meso-mechanics approach that considers the more detailed physical aspects of moisture ingress into a micro-cracked laminate is presented elsewhere (Roy and Bandorawalla, 1999).

The material influence coefficients needed to model the effect of bi-axial matrix micro-cracking on laminate diffusivity and maximum saturation level were evaluated by using hygrothermal test data for a $[0/90/0/90]_s$ graphite/epoxy 5-harness satin textile composite. The moisture weight gain curves predicted by using a quadratic diffusivity–damage relation yielded good correlation with test data. While these observations do not conclusively prove that the laminate diffusivity and saturation level are indeed quadratic functions of crack density, it does indicate that retaining only up to the quadratic terms in damage in the expansion of the Gibbs potential is an acceptable modeling approximation for the material system under consideration. The primary purpose of this paper is to establish a theoretical framework for using the proposed modeling approach to characterize, and eventually, to predict absorption and desorption in biaxially micro-cracked laminates. The formulation presented in this paper is deemed to provide a small yet positive step towards that goal. Additional hygrothermal tests on specimens subjected to combined stress and damage states at different temperature and humidity levels are currently underway to comprehensively evaluate the accuracy of the proposed model when these data become available.

Acknowledgements

The authors are grateful to Dr. Rajiv Naik and Mr. Ron Cairo of Pratt & Whitney, and to Mr. Mike Meador of NASA Glenn Research Center for supporting this research. The authors would also like to thank Professor Ramesh Talreja of Georgia Tech. for his valuable suggestions. The Virginia Tech. authors would also like to acknowledge the support of the Air Force Office of Scientific Research and the National Science Foundation for their support under grant CMS-9872331.

References

Adkins, J.E., 1959. Symmetry relations for orthotropic and transversely isotropic materials. Arch. Rational Mech. Anal. 4, 193–213.

Carter, H.G., Kibler, K.G., 1978. Langmuir-type model for anomalous diffusion in composite resins. Journal of Composite Materials 12, 118–130.

Gurtin, M.E., Yatomi, C., 1979. On a model for two phase diffusion in composite materials. Journal of Composite Materials 13, 126–130.

Roy, S., Bandorawalla, T., 1999. Modeling of diffusion in a micro-cracked composite laminate using approximate solutions. Journal of Composite Materials 33 (10), 872–905.

Roy, S., Xu, W., 2001. Modeling of diffusion in the presence of damage in polymer matrix composites. International Journal of Solids and Structures 38, 115–125.

Shen, C.H., Springer, G.S., 1981. Effects of moisture and temperature on the tensile strength of composite materials. In: Springer, G.S. (Ed.), Environmental Effects on Composite Materials, Technomic Publishing Co., Inc., Lancaster, PA, pp. 79–93.

Shirrell, C.D., Leisler, W.H., Sandow. F.A., 1979. Moisture-induced surface damage in T300/5208 graphite/epoxy laminates. In: Pipes, R.B. (Ed.), Nondestructive Evaluation and Flaw Criticality for Composite Materials, ASTM STP 696, American Society for Testing and Materials, pp. 209–222.

Talreja, R., 1994. Damage characterization by internal variables. In: Talreja, R. (Ed.), Damage Mechanics of Composite Materials, Elsevier, Amsterdam, p. 53–78.

Weitsman, Y., 1987. Coupled damage and moisture transport in fiber-reinforced, polymeric composites. International Journal of Solids and Structures 23 (7), 1003–1025.

Weitsman, Y., 1991. Moisture in Composites: Sorption and Damage. In: Reifsnider, K.L., Fatigue of Composite Materials, Elsevier, Amsterdam, pp. 385–429.